Thermochemical Properties of Polycyclic Aromatic Hydrocarbons (PAH) from G3MP2B3 Calculations

Guillaume Blanquart* and Heinz Pitsch

Department of Mechanical Engineering, Stanford University, Stanford, California 94305

Received: December 13, 2006; In Final Form: April 6, 2007

In this article, we present a new database of thermodynamic properties for polycyclic aromatic hydrocarbons (PAH). These large aromatic species are formed in very rich premixed flames and in diffusion flames as part of the gas-phase chemistry. PAH are commonly assumed to be the intermediates leading to soot formation. Therefore, accurate prediction of their thermodynamic properties is required for modeling soot formation. The present database consists of 46 species ranging from benzene (C_6H_6) to coronene ($C_{24}H_{12}$) and includes all the species usually present in chemical mechanisms for soot formation. Geometric molecular structures are optimized at the B3LYP/6-31++G(d,p) level of theory. Heat capacity, entropy, and energy content are calculated from these optimized structures. Corrections for hindered rotor are applied on the basis of torsional potentials obtained from second-order Møller-Plesset perturbation (MP2) and Dunning's consistent basis sets (cc-pVDZ). Enthalpies of formation are calculated using the mixed G3MP2//B3 method. Finally, a group correction is applied to account for systematic errors in the G3MP2//B3 computations. The thermodynamic properties for all species are available in NASA polynomial form at the following address: http://www.stanford.edu/group/pitsch/.

I. Introduction

The formation of polycyclic aromatic hydrocarbons (PAH) is a key issue in the understanding of soot formation. Soot is formed in many industrial devices such as furnaces, but also in automotive and aircraft engines and in fires. Soot has become a major concern for public health and the environment. It is commonly assumed that the inception of soot particles occurs by the collision of heavy PAH.[1] The particles further grow by coalescence with other particles or by addition of mass on the surface through chemical reactions. Most models consider that incipient molecules originate in benzene and grow by addition of carbon atoms following the H-abstraction C_2H_2-addition mechanism (HACA).[2] However, the size and type of those molecules differ from model to model.[3−5] During the growth by chemical reactions, additional six-membered rings as well as new five-membered rings are formed. These five-membered ring molecules, commonly referred to as cyclopentafused PAH (CP-PAH), are formed generally by direct cyclization after addition of acetylene (C_2H_2) on radicals like naphthyl. However, the same reaction of acetylene addition can also lead to stable ethynyl-substituted aromatics. In a flame, an equilibrium is established quickly between the CP-PAH and the ethynyl-substituted aromatics. Recent work by Marsh and Wornat[6] shows that CP-PAH should be formed preferentially in comparison to the ethynyl-substituted aromatics when the path is available. Also, branching ratios have been found to be largely in favor of the direct cyclization reaction at high temperature and for a wide range of pressures.[7] Those results suggest that the main path from benzene to higher PAH involves the formation of acenaphthylene and other CP-PAH. While the path to form acenaphthylene from naphthalene was included in some of the recent soot mechanisms,[8] growth beyond acenaphthylene to form larger CP-PAH (like acephenanthrylene or cyclopenta-[cd]pyrene) was not considered. However, adding this path to existing reaction mechanisms is not straightforward because of the lack of kinetics and thermodynamic properties.

The evolution of PAH from benzene up to the nucleation into soot particles is typically described using detailed chemical kinetic reaction mechanisms. Modeling soot formation therefore requires the knowledge of the underlying PAH chemistry, which itself relies on the thermodynamic properties of the aromatic species. A quite comprehensive database of thermodynamic properties of PAH has been developed by Wang and Frenklach.[9] They used the AM1 level of theory with additional group corrections to predict the enthalpies of formation. While their database is already extensive, it does not include cyclopentafused molecules above acenaphthylene ($C_{12}H_8$). Wang and Frenklach[9] also noted some inaccuracies in predictions of the vibrational frequencies used for the computation of heat capacities and entropies. Finally, the planarity of some of the molecules was not discussed, and corrections for internal degrees of rotation (hindered rotors) were not included.

The intent of the present work is to develop a new database for thermodynamic properties of PAH that expands the range of molecules considered by Wang and Frenklach[9] and which overcomes the other above-mentioned shortcomings. This database will include molecules both with and without five-membered rings. The species are chosen on the basis of their relevance for soot formation mechanisms. Geometric structures are first optimized at various levels of theory and with various basis sets. The shapes of the molecules as well as their planarity are discussed. Molecules with internal degrees of freedom are further analyzed, and torsional potentials are derived. From the best optimized geometric structure (B3LYP/6-31++G(d,p)), thermodynamic properties such as heat capacity and entropy are derived. Then, the enthalpies of formation of these species are computed with the mixed method G3MP2//B3. Finally, a

* Corresponding author. E-mail: gblanqu@stanford.edu. Ph: 1 650 723 4503. Fax: 1 650 725 3525.

10.1021/jp068579w CCC: $37.00 © 2007 American Chemical Society
Published on Web 06/27/2007

TABLE 1: Bond Length (in Å) for the Benzene Molecule Computed with Various Levels of Theory and Basis Sets

theory	basis set	C−H	C−C
HF	6-31G(d)	1.0755	1.3863
B3LYP	6-31G(d)	1.0870	1.3968
	6-311++(d,p)	1.0844	1.3947
MP2	cc-pVDZ	1.0952	1.4057
	cc-pVTV	1.0814	1.3937
	cc-pVQZ	1.0808	1.3911
exptl		1.084	1.397

group correction is applied to improve the accuracy of the computed energies.

II. Geometric Structures

Computational Method. The geometric molecular structures are optimized iteratively, with each iteration using an increased level of theory to refine the solution toward the optimum. The first optimization uses the Hartree Fock (HF) method and the 6-31G(d) basis set. The HF method is the simplest ab initio calculation that can be performed. However, it is not accurate enough for the computation of vibrational frequencies.

Next, the B3LYP[10,11] functional is used with the same basis set. This functional accounts for some electron correlation through empirical correlation terms and has been widely used for optimization of geometric structures. While the functional might not be accurate enough for the prediction of the energy barrier between geometric structures, the results are usually considered reliable enough for the computation of the thermodynamic properties, such as heat capacity, entropy, and energy content. Finally, the 6-311++G(d,p) basis set,[12] which includes diffuse and polarization functions, is used with B3LYP to ensure even more accurate predictions of the properties.

To ascertain the quality of the proposed method (B3LYP functional with 6-311++G(d,p) basis set), the benzene molecule is studied in greater detail. The geometric structure of this representative aromatic species is optimized using the Møller−Plesset perturbation formalism (MP2), which represents the logical next step in the refinement of the level of theory. This level of theory combined with the Dunning correlation consistent basis sets (cc-pVDZ, cc-pVTZ, and cc-pVQZ) offers predictions of higher fidelity for the C−H and C−C bond lengths in the benzene molecule.

All calculations were performed using the *Gaussian 03* computer program.[13]

Results. First, the C−C and C−H bond lengths of the benzene molecule are computed from the various levels of theory. The results are available in Table 1 and are compared with experimental data.[14] The HF method clearly underestimates the bond lengths. The MP2 methods converges to values slightly lower than the experimental values as the size of the basis set is increased from cc-pVZD to cc-pVTZ and then cc-pVQZ. On the other hand, the B3LYP functional with the 6-311++(d,p) basis set predicts both the C−H and the C−C bond lengths with good accuracy.

The list of species considered in the present work is given in Table 2. Here, only the symmetry group of the molecules is included as geometric structure information. Full geometric structures are available as part of the Supporting Information. To simplify discussions of the species, the nomenclature introduced by Frenklach et al.[15] is used. Following this nomenclature, aromatic rings are represented by the letter A. The following subscript corresponds to the number of aromatic rings in the molecule. If the molecule is substituted, the groups are placed thereafter. For example, $A_1C_2H_3$ means one aromatic ring with a vinyl group attached to it.

Most of the PAH are planar under the present conditions and show at least C_s group symmetry at the three levels of theory considered. Because of an internal degree of freedom, some PAH are not planar. The geometric structure of those molecules will be discussed later. Other PAH are not planar even in the absence of internal degrees of rotation. This is the case for the vinyl-substituted phenanthrene and acephenanthrylene ($A_3C_2H_2$ and $A_3R5C_2H_2$). These molecules require further attention. The lowest-energy optimal structures for these molecules are found to be nonplanar for all levels of theory considered, as shown in Figure 1. The optimal structure of vinyl phenanthrene obtained with B3LYP/6-311++G(d,p) exhibits a maximum dihedral angle of about 27°. In fact, both of these molecules have two optimal structures corresponding to a mirror image of one another. An optimal planar structure for those molecules exists, but a vibrational frequency analysis reveals one negative frequency, characteristic of saddle points. The planar structures separate the optimal structures with positive and negative dihedral angles. In the case of vinyl phenanthrene, the energy barrier between these two optimal structures was calculated and was found to be about 28.77 kJ/mol with HF/6-31G(d) and 30.84 kJ/mol with B3LYP/6-311++G(d,p). Using a Boltzmann distribution, one can estimate the equilibrium distribution of vinyl phenanthrene. Under normal flame conditions ($T = 1500$ K), the planar structure is barely populated at less than 10%.

In contrast to these structures, the two ethynyl-substituted phenanthrene and acephenanthrylene molecules (A_3C_2H and A_3R5C_2H) are planar for the three levels of theory considered. Because of the strong nonplanarity of the vinyl-substituted molecules, a greater emphasis was put on the geometric structure of the two ethynyl-substituted molecules. In the attempt to find a nonplanar optimal configuration, several optimizations were performed with different starting points and with different convergence methods. For all simulations, the final optimal point always corresponded to a planar molecule, and it was not possible to recover a configuration similar to the vinyl-substituted molecules. Furthermore, a sensitivity analysis on the optimal structure did not reveal negative frequencies, hence confirming that this optimum was indeed a minimum.

III. Torsional Potential

Computational Method. Some molecules like the vinyl-substituted PAH exhibit an internal degree of freedom. This internal degree of freedom corresponds to an internal torsion where a section of the molecule can rotate with respect to the rest of the molecule. To better determine the ground-state torsional angle between those two parts, a more thorough analysis of the torsional potential is required. The intent of the present work is to find reasonable estimates for the ground-state torsional angle as well as the energy barrier to rotation. Functionals like B3LYP are known to be unable to accurately reproduce the torsional potential of molecules like styrene.[16,17] On the other hand, methods like CC (coupled cluster), while very expensive, have been found to predict quite accurately the torsional potential.[16] In the present work, we chose to use the second-order Møller−Plesset perturbation formalism (MP2). This method fills the gap between the inaccurate B3LYP and the very expensive CC methods and has been used widely for computations of torsional potentials of substituted aromatic hydrocarbons.[16−18]

Both B3LYP and MP2 calculations are performed using the Dunning correlation consistent basis sets. In the scope of the

TABLE 2: Details of Optimized Molecules at B3LYP/6-311++G(d,p)

species		symmetry group	geometrical representation
name	formula		
benzene	A_1	D_{6h}	
phenyl radical	A_1-	C_{2v}	
ethynylbenzene	A_1C_2H	C_{2v}	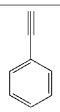
2-ethynylphenyl	A_1C_2H-2	C_s	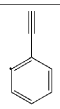
3-ethynylphenyl	A_1C_2H-3	C_s	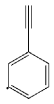
4-ethynylphenyl	A_1C_2H-4	C_{2v}	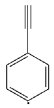
styrene	$A_1C_2H_3$	C_s	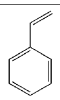
1-phenylvinyl	$i-A_1C_2H_2$	C_{2v}	
2-phenylvinyl	$n-A_1C_2H_2$	C_s	
1-vinyl-2-phenyl	$A_1C_2H_3*$	C_s	
1,2-diethynylbenzene	$A_1(C_2H)_2$	C_{2v}	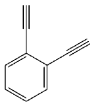
naphthalene	A_2	D_{2h}	
1-napthhyl	A_2-1	C_s	
2-napthhyl	A_2-2	C_s	
2-ethynylnaphthalene	A_2C_2HB	C_s	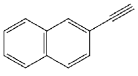
2-ethynyl-1-naphthyl	A_2C_2HB*	C_s	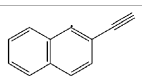
1-ethynylnaphthalene	A_2C_2HA	C_s	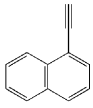

species		symmetry group	geometrical representation
name	formula		
1-ethynyl-2-naphthyl	A_2C_2HA*	C_s	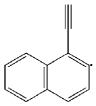
vinylnaphthalene	$A_2C_2H_3$	C_1	
2-naphthylvinyl	$A_2C_2H_2$	C_1	
1,2-diethynylnaphthalene	$A_2(C_2H)_2$	C_s	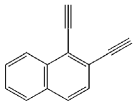
acenaphthylene	A_2R5	C_{2v}	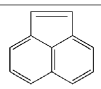
acenaphthyl	A_2R5-	C_s	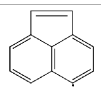
1-ethynylacenaphthylene	A_2R5C_2H	C_s	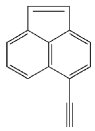
2-ethynyl-1-acenaphthyl	A_2R5C_2H*	C_s	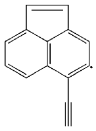
1,2-diethynylacenaphthylene	$A_2R5(C_2H)_2$	C_s	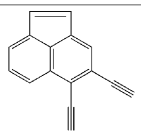
2-acenaphthylvinyl	$A_2R5C_2H_2$	C_1	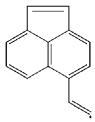
vinylacenaphthylene	$A_2R5C_2H_3$	C_1	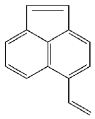
anthracene	A_3	D_{2h}	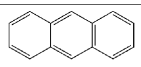
phenanphthrene	A_3	C_{2v}	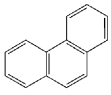
phenanphthryl	A_3-	C_s	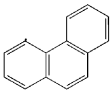
1-ethynylphenanphthrene	A_3C_2H	C_s	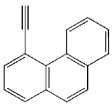

TABLE 2 (Continued)

species		symmetry group	geometrical representation
name	formula		
2-phenanphthrylvinyl	$A_3C_2H_2$	C_1	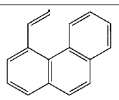
pyrene	$A_4(C_{16}H_{10})$	D_{2h}	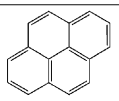
tetracene	$A_4(C_{18}H_{12})$	D_{2h}	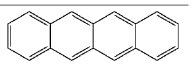
chrysene	$A_4(C_{18}H_{12})$	C_{2h}	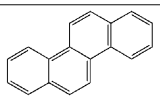
pyrenyl radical	A_4-	C_s	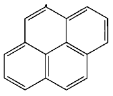
acephenanphthrylene	A_3R5	C_s	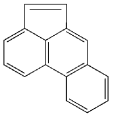
acephenanphthryl	A_3R5-	C_s	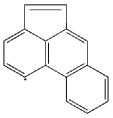

species		symmetry group	geometrical representation
name	formula		
1-ethynylacephenanphthrene	A_3R5C_2H	C_s	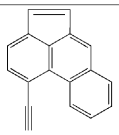
2-acephenanphthrylvinyl	$A_3R5C_2H_2$	C_1	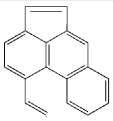
cyclopenta[cd]pyrene	A_4R5	C_s	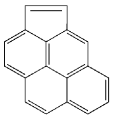
biphenyl	P_2	D_2	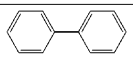
biphenyl radical	P_2-	C_1	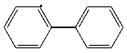
perylene	A_5	D_{2h}	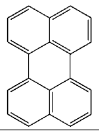
coronene	A_7	D_{6h}	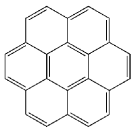

present work, using the second-order perturbation theory (MP2) with the first Dunning basis set (cc-pVDZ) was found to be a good compromise between accuracy and cost. To quantify the accuracy of this choice, the torsional potential of the styrene molecule is also computed using the next larger Dunning basis set: cc-pVTZ. However, it will be shown later that the small gain in accuracy does not justify the increase in calculation time. As a consequence, the torsional potentials of the other species are only computed at the MP2/cc-pVDZ level of theory.

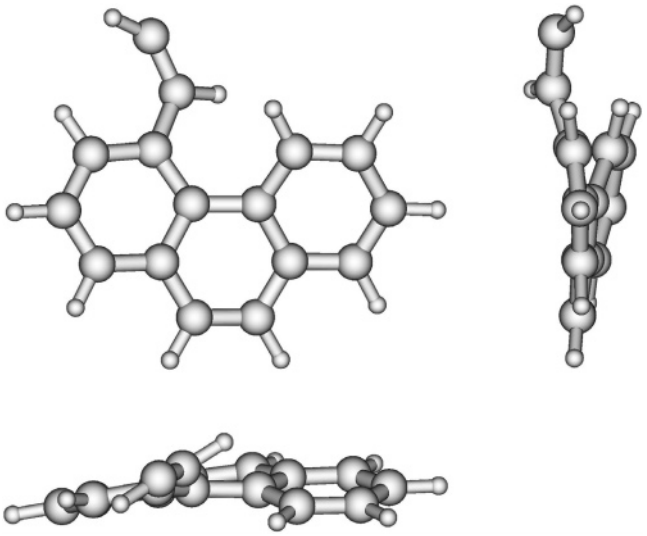

Figure 1. Geometric structure of vinyl phenanthrene ($A_3C_2H_2$) optimized with B3LYP//6-311++G(d,p).

The torsional potentials were obtained by increasing the torsional angle between the two rotating parts by increments of 15°. For each new configuration, the full geometry was reoptimized with the torsional angle kept frozen. Then, the energy was shifted with respect to the optimal configuration whose energy was set to zero.

Results. Figure 2 shows the predicted torsional potential of the styrene molecule ($A_1C_2H_3$) at three levels of theory: B3LYP/cc-pVDZ, MP2/cc-pVDZ, and MP2/cc-pVTZ. Also shown in the figure are the experimental measurements of the torsional potential by Caminati et al.[19] As expected, the second-order perturbation theory predicts the energy barrier as well as the

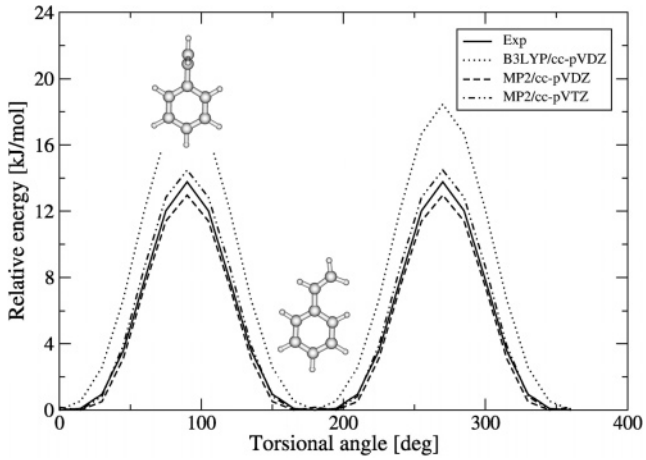

Figure 2. Predicted torsional potential of styrene with comparison to experimental measurements.[17]

TABLE 3: Ground-State Twist Angle (in deg) and Energy Barrier to Rotation (in kJ/mol) from Current B3/cc-pVDZ and MP2/cc-pVDZ Calculations

	twist angle		energy barrier	
species formula	B3LYP	MP2	B3LYP	MP2
$A_1C_2H_3$	0	18.8	18.5	13.0
$n - A_1C_2H_2$	0	89.6	21.8	10.8
$A_1C_2H_3$*	0	97.9	22.6	13.6
$A_2C_2H_3$	34.6	42.0	13.5	17.9
$A_2C_2H_2$	36.6	59.7	9.9	21.2
P_2	39.0	43.0	9.1	12.6
$P_2 -$	24.1	90.0	13.0	22.3

entire shape of the potential more accurately. While the second-order perturbation calculation with the cc-pVDZ basis set is slightly below the experimental measurements, the calculation with the larger cc-pVTZ basis set is slightly above. However, the deviations of those two results from the experimental data are the same, about 0.8 kJ/mol for the configuration where the vinyl group is perpendicular to the aromatic ring. As a consequence, the other torsional potentials are computed only with B3LYP/cc-pVDZ and MP2/cc-pVDZ.

The B3LYP method predicts the styrene molecule to be planar (C_s symmetry group), while the MP2 method both with cc-pVDZ and with cc-pVTZ predicts a nonplanar molecule (C_1 symmetry group). However, the energy difference between the planar and nonplanar configurations is very small, less than 0.2 kJ/mol at the MP2/cc-pVDZ level of theory. Because of this very shallow well, determining the equilibrium twist angle is difficult. Early experimental measurements[19] suggested a planar configuration, while results from recent electron diffraction studies[20] favor the nonplanar molecule with a twist angle of about 27°. The predictions of a nonplanar structure from the present MP2 calculations and other MP2[21] and CC results[17] are consistent with the last experimental observation. However, the prediction of the equilibrium twist angle of the nonplanar molecule is strongly dependent on the level of theory considered for the computation. With second-order perturbation theory (MP2), Moriarty et al.[21] found an equilibrium twist angle of 27.6° with a small basis set (6-31G(d)), while we obtained 18.8° with a medium-size basis set (cc-pVDZ) and 14.9° with a larger basis set (cc-pVTZ). With an even higher level of theory (CC/cc-pVDZ), Sancho-García and Pérez-Jiménez[17] obtained an angle of about 10.0°. While the molecule always remains nonplanar, the twist angle monotonically decreases as the quality of the method or the size of the basis set increases. From those observations, one could stipulate that the styrene molecule is not planar and that its equilibrium twist angle should be close to 10°. Table 3 summarizes the resulting twist angle and energy barrier to rotation with the two methods (B3LYP and MP2 with cc-pVDZ) for different molecules.

Two radicals of the styrene molecule are of special interest: 1-vinyl-2-phenyl ($A_1C_2H_3$*) with the radical site on the phenyl group and 2-phenylvinyl (n-$A_1C_2H_2$) with the radical site at the end of the vinyl group. As shown in Figure 3, both of these molecules exhibit an energy barrier to rotation similar to styrene. However, the molecules are not planar in their ground states, because of the interaction between the radical site and the rest of the molecule. For the two radicals, the MP2 calculations predict the rotating parts to be nearly orthogonal while the B3LYP method still predicts a planar molecule. For the 2-phenylvinyl, the twist angle is at 89.6° both with MP2/cc-pVDZ and with MP2/cc-pVTZ. The twist angle is slightly larger for 1-vinyl-2-phenyl with a value of 97.9° with MP2/cc-pVDZ and 104.1° with MP2/cc-pVTZ. In those computations, a zero twist angle corresponds to the vinyl group facing the radical

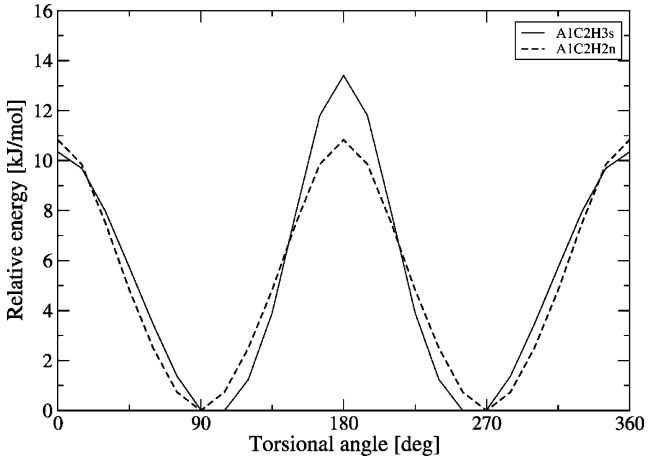

Figure 3. Predicted torsional potential of styrene radicals.

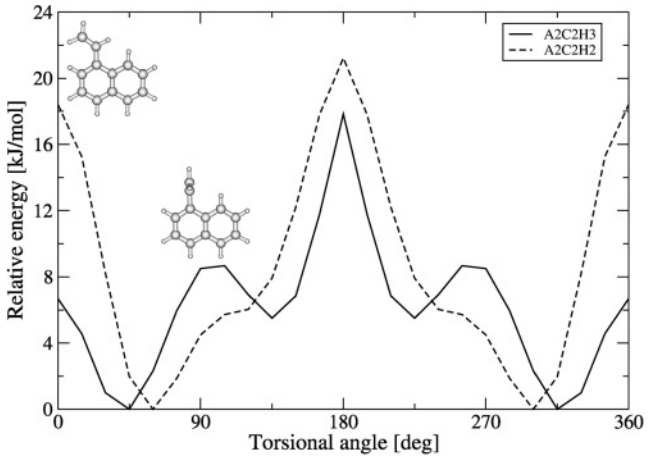

Figure 4. Predicted torsional potential of vinyl naphthalene.

site. Once again, it appears that the twist angle is a function of the size of the basis set. Moriarty et al.[21] optimized the geometric structures of 2-phenylvinyl and 1-vinyl-2-phenyl at several levels of theory and with different basis sets. Using small basis sets (from 3-21G to 6-31G(d,p)), they found smaller equilibrium twist angles for the two molecules than the present MP2 calculations: 38.1°for 2-phenylvinyl and 5.8° for 1-vinyl-2-phenyl with their highest level of theory (MP2/6-31G(d,p)).

Figure 4 shows the torsional potential for the vinyl naphthalene molecule ($A_2C_2H_3$) and radical ($A_2C_2H_2$). The starting point, referred to as zero twist angle, corresponds to the configuration where the molecule is planar with the vinyl group pointing away from the second aromatic ring. Because of the strong repulsion of the vinyl group with the second aromatic ring, neither of the molecules are predicted to be planar, even at the B3LYP level of theory. Since the molecule and the radical are not symmetric with respect to the rotation, the torsional potential does not exhibit the same periodic multiwell shape that was observed from the styrene molecule and radicals. The potential rather goes through several local minima and maxima.

Finally, Figure 5 shows the torsional potential for the biphenyl molecule and radical. The figure also shows the experimental potential measured by Bastiansen et al.[22] Experimental results[23] indicate a twist angle of about 44.4°, in very good agreement with the present MP2 computation (43.0°). The energy barrier to rotation was found from experiments to be around 6.0 ± 0.5 kJ/mol for the planar and ortho configurations.[22−24] The MP2 calculations predict an energy barrier of 12.5 kJ/mol for the ortho and 7.7 kJ/mol for the planar configurations. Tsuzuki et al.[18] performed similar MP2 calculations with larger basis sets

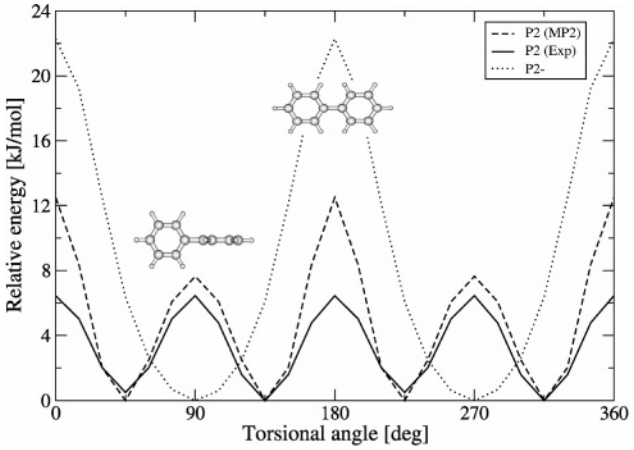

Figure 5. Predicted torsional potential of biphenyl and biphenyl radical.

TABLE 4: List of Species Selected to Compute the Scaling Factor Applied to the Theoretical Vibrational Frequencies

species name	species formula	number of frequencies
ethylene	C_2H_4	12
propargyl radical	C_3H_3	3
propyne	C_3H_4	10
allene	C_3H_4	11
cyclopropene	C_3H_4	15
phenyl radical	C_6H_5	26
benzene	C_6H_6	20
fulvene	C_6H_6	26
styrene	C_6H_8	38

as well as other methods like MP4 (fourth-order Møller−Plesset perturbation) and CCSD(T) (coupled cluster both single and double substitutions with perturbative estimation of the contributions of triple excitations). With these quite costly levels of theory, they were able to reproduce the energy barrier at 90°, but not the one at 0°. A more thorough analysis of this torsional potential with more accurate methods and larger basis sets should be considered to resolve these discrepancies. However, such analysis is beyond the scope of the present paper.

IV. Thermodynamic Properties

As mentioned earlier, the geometric structures and vibrational frequencies for all stationary points considered here were calculated using the B3LYP functional[10,11] and the 6-311++G-(d,p) basis set.[11] To improve the accuracy of the thermodynamic properties, such as specific heat capacity and entropy, the vibrational frequencies were rescaled using a common scaling factor. This scaling factor was evaluated from a least-squares approach by comparing experimental and computed frequencies as described by Scott and Radom.[25] A set of molecules relevant for the present study has been selected (Table 4), whose experimental vibrational frequencies were taken from the Computational Chemistry Comparison and Benchmark Database (NIST).[26] The set of molecules has been selected from the C_2, C_3, and C_6 species to represent the most important structural groups for the investigated PAH for which experimental data are available. The fitted scaling factor for the computed vibrational frequencies with respect to their experimental frequencies is 0.96626, with a relative uncertainty of ±0.0102. The heat capacity $C_p^\circ(T)$, entropy $S^\circ(T)$, and thermal energy content $H^\circ(T) - H^\circ(0)$ were computed using the rescaled vibrational frequencies and the moments of inertia. Table 5 summarizes the thermodynamic properties for all species.

Some of the molecules have one internal degree of rotation. This internal rotation is treated as a hindered rotor rather than as a free rotor for better prediction of the thermodynamic properties. Correcting the thermodynamic properties for hindered rotors requires the computation of the torsional potential of the molecule. The torsional potentials for some of these molecules were presented in the previous section. Due to the inherent cost of the computations, the torsional potentials were only evaluated for a set of molecules whose rotating tops are representative of those typically found in PAH. Then, it is assumed that two molecules with identical rotating tops have identical torsional potentials. For instance, the torsional potentials of the molecules $A_2C_2H_2$ and $A_2R5C_2H_2$ are assumed to be identical, because the rotating tops are the same. However, the rotating top found in those two molecules ($A_2C_2H_2$ and $A_2R5C_2H_2$) is different from the one found in *n*-$A_1C_2H_2$ because of the presence of the second aromatic group. This restriction is justified by the localized interaction between the vinyl group and the closest atoms of the remaining part of the molecule.

To simplify the treatment of the internal rotation as hindered rotors, Pitzer et al.[27] originally assumed that the torsional potential follows the relation

$$V(\varphi) = \frac{1}{2} V_0[1 - \cos(n\varphi)] \qquad (0.1)$$

with V_0 the barrier to rotation, n the number of wells of the potential, and $\phi = 0$ the location of the minimum. However, it can be observed in Figures 2−5 that the torsional potentials of several of the PAH do not follow this relation. In fact, this restriction is equivalent to considering only the most energetic mode in the Fourier series expansion of the torsional potential function. In the present work, we follow the more accurate approach of Lay et al.[28] The potential function is decomposed into its Fourier modes

$$V(\varphi) = a_0 + \sum_k a_k \cos(k\varphi) + \sum_k b_k \sin(k\varphi) \qquad (0.2)$$

Then, an approximate Hamiltonian matrix is formed by evaluating the Hamiltonian operator on a given set of wave functions of free rotation (100 wave functions are used in the present work). The energy levels of a molecule are obtained by diagonalization of the Hamiltonian matrix. Then, the thermodynamic properties are evaluated from these energy levels. A Fortran program, *ROTATOR*,[28] is used for the discretization of the Hamiltonian operator and calculation of the energy levels. Finally, the degeneracy of the energy levels is included in the partition function by considering the ratio of the periodicity of the potential to the symmetry number of the rotating top.

Table 6 lists the heat capacity and entropy for some of the molecules with internal degree of rotation. Three sets of thermodynamic properties have been computed. In the first set, the internal rotation was treated as a simple vibration, thus equivalent to not applying any corrections. In the second set, the internal rotation was treated as a free rotor, while a correction for hindered rotor was used in the last set. Pitzer[29] measured the entropy for the styrene molecule at 298 K and obtained $S^\circ = 345.1 \pm 2.1$ kJ/mol. The entropy predicted without correction ($S^\circ = 355.4$ kJ/mol) is clearly overestimated, as is the entropy with correction for free rotor ($S^\circ = 350.1$ kJ/mol). On the other hand, correcting for hindered rotor leads to a value of $S^\circ = 345.7$ kJ/mol, which is within the margin of error of the experimental value. More recently, Chirico[30] measured the entropy of biphenyl and obtained $S^\circ = 389.7 \pm 0.3$ kJ/mol, which is very close to the value of $S^\circ = 391.7$ kJ/mol computed with correction for hindered rotor. Those results emphasize the

TABLE 5: Thermodynamic Properties of PAH Molecules at 298 K[a]

species formula	C_p°	S°	ΔH°	species formula	C_p°	S°	ΔH°
A_1	83.5	269.9	14.4	A_2R5C_2H	188.6	410.1	29.3
A_1-	82.0	289.8	14.4	A_2R5C_2H*	186.9	416.4	29.3
A_1C_2H	117.6	329.8	19.9	$A_2R5(C_2H)_2$	223.3	454.6	35.3
A_1C_2H-2	116.0	341.4	19.9	$A_2R5C_2H_2$	195.2	429.1	30.6
A_1C_2H-3	116.0	340.7	19.8	$A_2R5C_2H_3$	196.7	424.5	30.8
A_1C_2H-4	115.9	334.7	19.8	A_3	185.9	391.7	28.3
$A_1C_2H_3$	120.8	345.7	20.4	A_3	185.5	398.5	28.3
$i-A_1C_2H_2$	124.7	350.0	21.5	A_3-	183.6	408.6	28.2
$n-A_1C_2H_2$	123.0	350.1	21.0	A_3C_2H	219.7	454.1	34.2
$A_1C_2H_3$*	121.1	357.1	20.9	$A_3C_2H_2$	222.4	455.9	34.4
$A_1(C_2H)_2$	152.0	374.7	25.6	$A_4(C_{16}H_{10})$	203.8	402.9	30.1
A_2	134.4	335.3	21.1	$A_4(C_{18}H_{12})$	237.7	448.2	35.6
A_2-1	132.8	352.3	21.0	$A_4(C_{18}H_{12})$	236.9	456.5	35.7
A_2-2	133.0	352.1	21.0	A_4-	201.9	419.8	30.0
A_2C_2HB	168.7	392.0	26.8	A_3R5	205.7	422.0	30.8
A_2C_2HB*	166.9	398.4	26.9	A_3R5-	203.9	427.2	30.7
A_2C_2HA	168.5	391.0	26.8	A_3R5C_2H	239.8	467.0	36.6
A_2C_2HA*	166.8	396.9	26.8	$A_3R5C_2H_2$	240.5	472.3	36.7
$A_2C_2H_3$	176.5	405.9	28.2	A_4R5	224.0	433.0	32.7
$A_2C_2H_2$	174.9	410.4	28.0	P_2	167.6	391.7	26.9
$A_2(C_2H)_2$	202.9	435.3	32.7	P_2-	165.0	401.1	26.8
A_2R5	154.7	359.9	23.5	A_5	255.6	469.2	38.0
A_2R5-	152.5	370.7	23.4	A_7	287.9	472.0	41.2

[a] Heat capacities and entropies are in J/mol/K; enthalpies are in kJ/mol.

TABLE 6: Comparison of Heat Capacity and Entropy with and without Correction for Internal Rotations[a]

	degeneracy		C_p°			S°		
species formula	σ	π	no correction	free rotation	hindered rotation	no correction	free rotation	hindered rotation
$A_1C_2H_3$	1	2	121.9	117.7	120.8	355.4	350.1	345.7
$n-A_1C_2H_2$	1	2	121.9	117.8	123.0	348.7	354.9	350.1
$A_1C_2H_3$*	1	1	120.1	116.0	121.1	349.2	362.3	357.1
$A_2C_2H_3$	1	1	172.7	168.6	176.5	397.7	411.8	405.9
$A_2C_2H_2$	1	1	172.3	168.2	174.9	404.2	417.6	410.4
P_2	2	2	167.0	162.9	167.5	385.1	396.2	391.7
P_2-	1	2	165.5	161.4	165.0	404.7	407.5	401.1

[a] Corrections include free rotor and hindered rotor. The symmetry number of the rotating top (σ) and the periodicity of the potential are also given. Heat Capacities and entropies are in J/mol/K.

importance of treating internal degrees of rotation in PAH as hindered rotors, and not only as free rotor.

V. Enthalpies of Formation

G3MP2//B3 Method. The enthalpies of formation of all considered species were calculated using the G3(MP2)//B3LYP method, which is based on ab initio calculations, and empirically based corrections. Full details, the theoretical basis, and a validation of the method can be found in Baboul et al.[31] Here, only a brief description is provided.

In the first step of the method, the geometries are optimized at the B3LYP/6-31G(d) level. The zero-point energies (ZPE) are obtained from this level and scaled by a factor of 0.96. In the second step, a single-point quadratic configuration interaction with triples is performed using the frozen core approximation, QCISD(T,FC)/6-31G(d). In the third step, a second-order Møller−Plesset perturbation theory computation is done on the original basis set MP2/6-31G(d) and on a larger basis set denoted MP2/G3MP2Large. This last basis set corresponds to 6-311+G-(2df,2p) for second-row elements. Finally, the method of Baboul et al.[31] applies a so-called higher-level correction (HLC) to account for remaining deficiencies in the energy calculations. This correction is a linear function of the number of valence electrons (n_α, n_β)

$$E(\mathrm{HLC}) = -An_\alpha - B(n_\alpha - n_\beta) \qquad (0.3)$$

with $n_\alpha \geq n_\beta$. The values for A and B provided for molecules are 10.041 and 4.995 mE_h, respectively. From this, the corrected energy can be expressed as

$$E_0[\mathrm{G3(MP2)//B3}] = E(\mathrm{ZPE}) + E[\mathrm{QCISD(T)/6\text{-}31G(d)}] + E[\mathrm{MP2/G3MP2Large}] - E[MP2/\mathrm{6\text{-}31G(d)}] + E(\mathrm{HLC}) \qquad (0.4)$$

The standard heat of formation is then computed from the decomposition of the different species to hydrogen and carbon atoms in their standard state of reference. The heat of formation and energy content for the hydrogen and carbon atoms were taken from the NIST-JANAF tables.[32]

Group Correction. Some differences exist between the enthalpies of formation of the different species calculated in the present study and their experimental values. In order to improve the prediction of these enthalpies, the group correction method, originally developed by Wang and Frenklach,[9] is applied to the G3MP2//B3 computed values. The method is based on the idea that the deviations between computed and experimental enthalpies are systematic and that the errors in the enthalpies of formation of all molecules can be reconstructed from errors attributed to the different structural groups that define the molecules. From this assumption, the values for corrections associated with the structural groups appearing in the considered molecules can be determined. The subsequent evaluation of the corrected enthalpies is straightforward. Here,

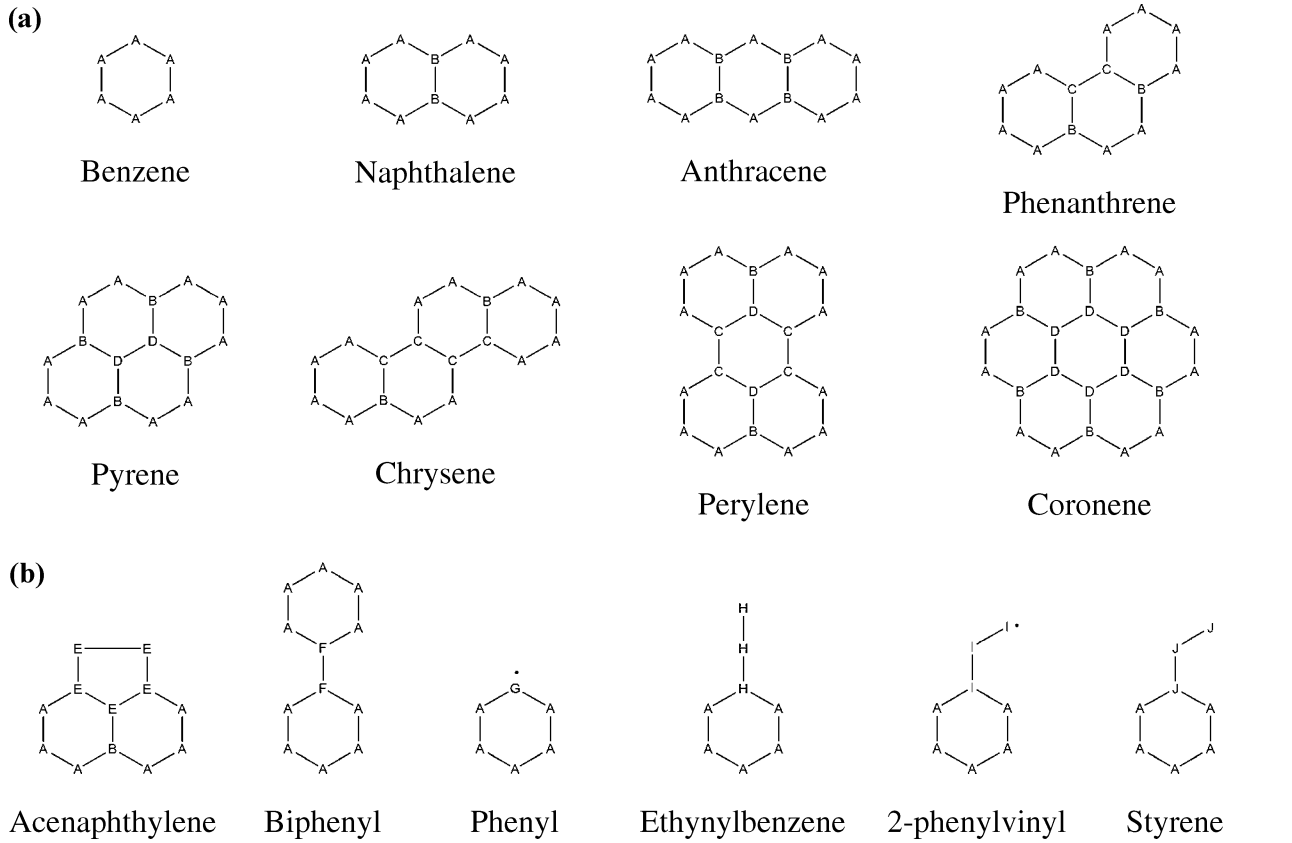

Figure 6. Geometric structures and group identification for the selected aromatic species used for determination of group corrections (A = C_B − H, B = C_F − $(C_B)_2(C_F)$, C = C_F − $(C_B)(C_F)_2$, D = C_F − $(C_F)_3$). (a) First set of structural groups. (b) Second set of structural groups.

we will first define the individual structural groups. Depending on the availability and reliability of experimental data for the molecules containing these groups, different methods will be used for the determination of the group correction values. Each of these will be detailed in the following, and an example for the validity of the structural group correction approach will be provided.

The structural groups used to define the considered molecules follow the definition of Benson[33] and can be categorized into two sets. The first set consists of four structural groups, which are found in purely aromatic species. This set is given by A = C_B − H, B = C_F − $(C_B)_2(C_F)$, C = C_F − $(C_B)(C_F)_2$, and D = C_F − $(C_F)_3$. Figure 6 shows the definition of the molecules that will be used below to determine the correction values for these groups. This figure also explains the structure of these four groups more clearly. The second set has six more groups found in substituted aromatics and radicals. This set is given by E = R5, and F = C_P − C_P, G = C ∗, H = C − C_2H, I = C − C_2H_2, and J = C − C_2H_3. Group E denotes a five-membered ring, such as in acenaphthalene, and group F connects the aromatic rings in biphenyl. Groups G, H, I, and J are substituted aromatics.

We will first determine the group correction values of the first set and provide an example for the validity of the approach. The corrections for the second set are discussed thereafter.

The details of the group correction method can be found in Wang and Frenklach.[9] The correction values for the groups are determined by comparing the computed enthalpies of formation for experimentally well characterized species with measured data and optimizing the required corrections for the structural groups by using a least-squares approach. For groups found in purely aromatic species, Wang and Frenklach[9] considered two sets of species in their least-squares method: a short list of five species and a larger list of eleven species. Their results showed that species used in the least-squares minimization have to be chosen carefully, because the energies of some molecules might suffer from large experimental uncertainties. Furthermore, the groups found in different species might not be identical. For these reasons, experimental values for different species cannot always be reproduced simultaneously with good accuracy. In our study, we chose to consider an intermediate list of eight species, which, according to the presently available chemical mechanisms for soot precursors, are all relevant for soot formation. This set consists of benzene, naphthalene, anthracene, phenanthrene, pyrene, chrysene, perylene, and coronene. Since all these molecules are constructed only from the four groups in the first set described above, only four parameters can be adjusted, and the system is overdetermined. A weighted least-squares minimization with the objective function

$$J(\mathrm{GC}_i) = \sum_{k=1}^{8} \left(\frac{\Delta_f H^\circ_{\mathrm{exp}} - \Delta_f H^\circ_{\mathrm{cal}} - \sum_{i=1}^{n_k} \mathrm{GC}_i}{\sigma_k} \right)^2 \qquad (0.5)$$

was used to determine the correction values GC_i of the structural group *i*. The weights σ_k represent the experimental error in the enthalpy of formation of species *k* at 298 K, $\Delta_f H^\circ_{\mathrm{exp}}$ are the experimental enthalpies of formation, and $\Delta_f H^\circ_{\mathrm{cal}}$ are the calculated G3(MP2)//B3 enthalpies.

The validity of the structural group correction approach and the accuracy of the values obtained for the first set of groups can be assessed for a simple example that involves only a few species. For this, we will consider a set of linear aromatic species of increasing size, including benzene (one ring), naphthalene

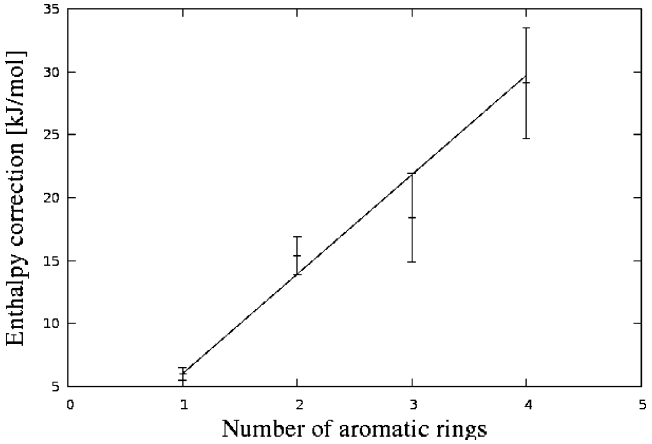

Figure 7. Required corrections to the computed enthalpies of formation for linear aromatic species: benzene (one ring), naphthalene (two rings), anthracene (three rings), and tetracene (four rings). Error bars correspond to the experimental uncertainties and the solid line to the group corrections from the present method.

(two rings), anthracene (three rings), and tetracene (four rings). Benzene consists of six $C_B - H$ groups. The three remaining species can be constructed from this by the successive addition of two $C_B - H$ and two $C_F - (C_B)_2(C_F)$ groups for each ring. This implies that the correction for these species can be written as

$$6GC_A + 2(r - 1)(GC_A + GC_B) \qquad (0.6)$$

where GC_A and GC_B are the correction values for the respective groups, and r is the number of aromatic rings. The correction is hence linear in the number of rings. Figure 7 shows the corrections to the computed values that are required to predict the lower and upper bounds of the experimental error margin. The solid line shows the corrections determined from the structural group correction values from the least-squares fitting procedure. It is observed that the linear trend for the corrections is found in the experimental data and that the structural group model provides the required corrections with reasonable accuracy.

While it is possible to find experimental measurements of the enthalpies of formation of different aromatic species with identical structural groups, experimental data are scarce for the substituted aromatics and radicals necessary to determine the correction values for the structures in the second set. Here, we have chosen one experimental data point for each of the structural groups. Experimental data are available for acenaphthylene, biphenyl, phenyl, ethynylbenzene, and styrene. These have been used in combination with the correction values of the first set of groups to determine the corrections for R5, $C_P - C_P$, C $*$, $C - C_2H$, and $C - C_2H_3$, respectively. For the remaining group, $C - C_2H_2$, no experimental enthalpies are available. Here, we use the phenylvinyl radical to determine the correction for $C - C_2H_2$ and determine the target enthalpy for this species from the experimental value for styrene and the bond dissociation energy (BDE) obtained from the difference in experimental energies of ethylene and vinyl.

Results. The enthalpies of formation of the eight targets used for aromatic species are presented in Table 7, while the group corrections are presented in Table 8. Most of the enthalpies of formation of the polycyclic aromatic hydrocarbons are taken from Slayden and Liebman.[34] Benzene and naphthalene have well-established enthalpies of formation, which are given as 82.93 ± 0.5 kJ/mol[35] and 150.3 ± 1.5 kJ/mol,[36] respectively.

TABLE 7: Standard Heat of Formation ($\Delta_f H^\circ_{298K}$) of the Target Species Obtained from Experiments (exp.) and Originally Calculated with G3(MP2)//B3 (orig.) Used for the Calculation of the Group Corrections (GC) in kJ/mol

		G3MP2//B3	
species	exp.	orig.	GC
Aromatic Species			
benzene	82.93 ± 0.5	76.95	82.99
naphthalene	150.3 ± 1.5	134.89	148.83
anthracene	226.7 ± 3.5	208.28	230.11
phenanthrene	201.7 ± 2.9	185.18	201.76
pyrene	225.7 ± 1.2	200.69	226.09
chrysene	263.5 ± 4.5	240.64	259.86
perylene	306.0 ± 0.8	283.32	306.11
coronene	302.0 ± 8.0	251.99	292.43
avg. error		22.11	2.34
substituted aromatics and radicals			
phenyl	339.7 ± 2.0	341.14	
phenylacetylene	306.6 ± 1.7	307.97	
styrene	146.9 ± 1.0	138.38	
styryl	393.5 ± 7.0	402.80	
acenaphthylene	259.7 ± 4.6	244.18	
biphenyl	182.0 ± 0.7	163.33	

TABLE 8: G3MP2//B3 Group Correction (in kJ/mol)

group	correction
$C_B - H$	1.007
$C_F - (C_B)_2(C_F)$	2.939
$C_F - (C_B)(C_F)_2$	0.314
$C_F - (C_F)_3$	1.787
C$*$	−6.476
$C - C_2H$	−6.406
$C - C_2H_2$	−14.336
$C - C_2H_3$	2.564
R5	6.538
$C_P - C_P$	8.699

New high-precision measurements of the enthalpy of formation of anthracene have been performed recently by Nagano.[37] The enthalpy of combustion was measured to be $\Delta_c H^\circ = -7065.0 \pm 1.1$ kJ/mol. This value leads to an enthalpy of formation for the solid phase of $\Delta_f H^\circ_s = 126.7 \pm 2.1$ kJ/mol. This value is in good agreement with the previously used value of 127.4 ± 5.9 kJ/mol.[38] Using the sublimation enthalpy from Oja and Suuberg,[39] the enthalpy of formation for the gas phase is evaluated as $\Delta_f H^\circ_g = 226.7 \pm 3.5$ kJ/mol. Similar measurements were performed for phenanthrene.[40] The enthalpy of combustion was established at $\Delta_c H^\circ = -7048.7 \pm 0.9$ kJ/mol, leading to an enthalpy of formation for the gas phase of $\Delta_f H^\circ = 201.7 \pm 2.9$ kJ/mol. This value agrees well with previous measurements.[41]

Finally, the enthalpies of formation of chrysene, perylene, and coronene are used as reported by Slayden and Liebman.[34]

The G3MP2//B3 method with group correction shows an average deviation between experimental and calculated enthalpies of formation of about 2.34 kJ/mol. This value shows great improvement compared to the results obtained by Wang and Frenklach[9] of 5.9 and 6.3 kJ/mol for the two sets of target species. To the knowledge of the authors, PAH of the size of coronene have not been computed with such expensive level of theory as G3MP2//B3. Although the configuration of coronene is substantially different from the other target species, the group corrections can also be applied to this molecule with an error within the experimental uncertainty, which demonstrates the efficiency of the method. The standard enthalpies of formation of the other species are reported in Table 9.

During the compilation of the sets of target species, three additional molecules were investigated, namely, tetracene

TABLE 9: Standard Enthalpies of Formation Calculated with the G3(MP2)//B3 Method with and without Group Corrections (in kJ/mol)

formula	0 K	298 K	298 K + GC	formula	0 K	298 K	298 K + GC
A_1C_2H-2	592.65	582.95	574.10	A_2R5-	544.17	525.30	533.34
A_1C_2H-3	588.39	578.64	569.79	A_2R5C_2H	491.65	472.38	480.49
A_1C_2H-4	588.08	578.29	569.44	A_2R5C_2H*	776.91	761.89	762.51
$i-A_1C_2H_2$	380.58	364.07	354.77	$A_2R5(C_2H)_2$	721.72	706.31	707.00
$n-A_1C_2H_2$	419.89	402.80	393.50	$A_2R5C_2H_2$	614.17	591.94	592.12
$A_1C_2H_3$*	427.99	410.85	410.97	$A_2R5C_2H_3$	335.63	309.33	326.41
$A_1(C_2H)_2$	553.17	542.84	534.06	A_3-	507.05	482.40	491.49
A_2-1	441.98	422.86	429.31	A_3C_2H	457.98	433.00	442.16
A_2-2	440.70	421.58	428.03	$A_3C_2H_2$	600.64	571.70	572.93
A_2C_2HB	385.33	365.70	372.22	A_4-	547.79	522.87	540.79
A_2C_2HB*	678.57	663.19	662.23	A_3R5	314.97	286.62	304.78
A_2C_2HA	383.90	364.20	370.72	A_3R5-	603.82	579.64	590.32
A_2C_2HA*	675.71	660.25	659.29	A_3R5C_2H	553.71	529.08	539.83
$A_2C_2H_3$	230.09	203.35	218.84	A_4R5	342.53	313.93	334.38
$A_2C_2H_2$	512.51	489.83	488.48	P_2-	469.22	445.25	456.54
$A_2(C_2H)_2$	613.80	597.87	596.98				

($C_{18}H_{12}$), triphenylene ($C_{18}H_{12}$), and pyracylene ($C_{14}H_8$). However, these molecules were not included in the least-squares approach, because of the uncertainty or scarcity of the experimental measurements. Measurements were performed for tetracene using the same methodology as for phenanthrene.[40] The enthalpy of combustion was established at $\Delta_cH° = -9005.1 \pm 1.8$ kJ/mol, thus leading to an enthalpy of formation for the gas phase of $\Delta_fH°_g = 331.6 \pm 4.4$ kJ/mol. While the value for phenanthrene agrees well with other measurements,[41] the value for tetracene is too endothermic. In earlier work, Slayden and Liebman[34] recommended a lower value for the enthalpy of formation for the gas phase of 302 kJ/mol. The present method using G3MP2//B3 predicts an enthalpy of formation of 287.68 kJ/mol without corrections and 317.40 kJ/mol with group corrections. This last value is very close to the arithmetic mean between the larger value of Nagano[40] and the recommended value of Slayden and Liebman,[34] 316.8 kJ/mol. This last value was used in Figure 7.

The computed enthalpies of formation of triphenylene are $\Delta_fH° = 239.99$ kJ/mol without correction and $\Delta_fH° = 253.96$ kJ/mol with correction. Slayden and Lienman[34] reported an enthalpy of formation of $\Delta_fH° = 265.5 \pm 2.5$ kJ/mol. Wang and Frenklach[9] already noticed that obtaining a good agreement between experimental and computed values for this molecule was difficult. They also noticed that the introduction of triphenylene in the least-squares approach would greatly lower the quality of the corrections.

The computed enthalpies of formation of pyracylene are $\Delta_fH° = 409.0$ kJ/mol without correction and $\Delta_fH° = 426.1$ kJ/mol with correction. An experimental measurement of the enthalpy of formation has been reported recently by Diogo et al.[42] with a value of $\Delta_fH° = 409.0 \pm 6.2$ kJ/mol. In this specific case, the method seems to perform better without the group corrections. However, as for triphenylene, the lack of repeated measurements with high accuracy justifies the removal of these two species from the least-squares optimization. Furthermore, these species typically do not appear in chemical mechanisms used to simulate soot formation.

VI. Conclusion

In this article, we have presented the thermodynamic properties and enthalpies of formation of an extensive set of polycyclic aromatic hydrocarbons relevant to soot formation. The geometric structures were optimized at different levels of theory, Hartree−Fock and B3LYP, using different basis sets, 6-31G(d) and 6-311++G(d,p). Results indicate that most of the species are planar under normal conditions. However, certain molecules exhibit an internal degree of rotation. A thorough analysis of the torsional potentials of those molecules has been performed. It was shown that treating those degrees of freedom as hindered rotor is necessary and that a sufficiently accurate level of theory is required to capture the energy barrier to rotation. Finally, the recent and expensive G3MP2//B3 method has been used to compute the enthalpies of formation of these species. We were able to extract group corrections to these enthalpies from a set of PAH molecules ranging from benzene up to coronene. The final corrected enthalpies show very good agreement with experimental data.

Acknowledgment. The authors gratefully acknowledge funding by the U.S. Department of Energy within the ASC program. The authors would also like to thank Masoud Aryanpour for his help with the *Gaussian 03* software.

Supporting Information Available: Optimized geometric structures of all species for all level of theory and basis sets mentioned in the present article. This material is available free of charge via the Internet at http://pubs.acs.org.

References and Notes

(1) Schuetz, C. A.; Frenklach M. *Proc. Combust. Inst*. **2002**, *29*, 2307−2314.
(2) Frenklach, M.; Wang, H. *Proc. Combust. Inst.* **1991**, *23*, 1559.
(3) Violi, A.; Sarofim, A. F.; Voth, G. A. *Combust. Sci. Technol*. **2004**, *176*, 991−1005.
(4) Wang, H.; Frenklach, M. *Combust. Flame* **1997**, *110*, 173−221.
(5) Mauss, F.; Trilken, B.; Breitbach, H.; Peters, N. In *Soot Formation in Combustion-Mechanism and Models*; Bockhorn, H., Ed.; Springer-Verlag: Berlin, 1994; pp 325−349.
(6) Marsh, N. D.; Wornat, M. J. *Proc. Combust. Inst*. **2000**, *28*, 2585−2592.
(7) Richter, H.; Mazyar, O. A.; Sumathi, R.; Green, W. H.; Howard, J. B.; Bozzelli, J. W. J. *Phys. Chem. A* **2001**, *105*, 1561−1573.
(8) Appel, J.; Bockhorn, H.; Frenklach, M. *Combust. Flame* **2000**, *121*, 122−136.
(9) Wang, H.; Frenklach, M. *J. Phys. Chem.* **1993**, *97*, 3867−3874.
(10) Becke, A. D. *J. Chem. Phys.* **1993**, *98*, 5648.
(11) Lee, C.; Yang, W.; Parr, R. G. *Phys. Rev. B.* **1988**, *37*, 785.
(12) Hehre, W. J.; L., R.; Pople, J. A.; Schleyer, P. v. R. *Ab Initio Molecular Orbital Theory*; Willey: New York, 1987.
(13) Frisch, M. J.; Trucks, G. W.; Schlegel, H. B.; Scuseria, G. E.; Robb, M. A.; Cheeseman, J. R.; Montgomery, J. A., Jr.; Vreven, T.; Kudin, K. N.; Burant, J. C.; Millam, J. M.; Iyengar, S. S.; Tomasi, J.; Barone, V.; Mennucci, B.; Cossi, M.; Scalmani, G.; Rega, N.; Petersson, G. A.; Nakatsuji, H.; Hada, M.; Ehara, M.; Toyota, K.; Fukuda, R.; Hasegawa, J.; Ishida, M.; Nakajima, T.; Honda, Y.; Kitao, O.; Nakai, H.; Klene, M.; Li, X.; Knox, J. E.; Hratchian, H. P.; Cross, J. B.; Bakken, V.; Adamo, C.; Jaramillo, J.; Gomperts, R.; Stratmann, R. E.; Yazyev, O.; Austin, A. J.; Cammi, R.; Pomelli, C.; Ochterski, J. W.; Ayala, P. Y.; Morokuma, K.;

Voth, G. A.; Salvador, P.; Dannenberg, J. J.; Zakrzewski, V. G.; Dapprich, S.; Daniels, A. D.; Strain, M. C.; Farkas, O.; Malick, D. K.; Rabuck, A. D.; Raghavachari, K.; Foresman, J. B.; Ortiz, J. V.; Cui, Q.; Baboul, A. G.; Clifford, S.; Cioslowski, J.; Stefanov, B. B.; Liu, G.; Liashenko, A.; Piskorz, P.; Komaromi, I.; Martin, R. L.; Fox, D. J.; Keith, T.; Al-Laham, M. A.; Peng, C. Y.; Nanayakkara, A.; Challacombe, M.; Gill, P. M. W.; Johnson, B.; Chen, W.; Wong, M. W.; Gonzalez, C.; Pople, J. A. *Gaussian 03*, revision C.01; Gaussian, Inc.: Wallingford, CT, 2004.

(14) Herzberg, G. *Electronic spectra and electronic structure of polyatomic molecules*; Van Norstrand: New York, 1966.

(15) Frenklach, M.; Clary, D. W.; Yuan, T.; Gardiner, W. C., Jr.; Stein, S. E.; *Combust. Sci. Technol.* **1986**, *50*, 79.

(16) Schmitt, M.; Ratzer, C.; Jacoby, C.; Leo Meerts, W. *J. Mol. Struct.* **2005**, *742*, 123−130.

(17) Sancho-Garcia, J.; Perez-Jimenez, A. J. *Phys. B: At. Mol. Opt. Phys.* **2002**, *35*, 1509−1523.

(18) Tsuzuki, A.; Uchimaru, T.; Matsumura, K.; Mikami, M.; Tanabe, K. J. *Chem. Phys.* **1999**, *110*, 2858−2861.

(19) Caminati, W.; Vogelsanger, B.; Bauder, A. *J. Mol. Spectrosc.* **1988**, *128*, 384−398.

(20) Cochran, J. C.; Hagen, K.; Paulen, G.; Shen, Q.; Tom, S.; Traeetteberg, M.; Wells, C. *J. Mol. Struct.* **1997**, *413*−*4*, 313−326.

(21) Moriarty, N. W.; Borwm, N. J.; Frenklach, M. *J. Phys. Chem. A* **1999**, *103*, 7127−7135.

(22) Bastiansen, O.; Samdal, S. *J. Mol. Struct.* **1985**, *128*, 115−125.

(23) Almenningen, A.; Bastiansen, O.; Fernholt, L.; Cyvin, B. N.; Cyvin, S. J.; Samdal, S. *J. Mol. Struct.* **1985**, *128*, 59−76.

(24) Carreira, L. A.; Towns, T. G. *J. Mol. Struct.* **1977**, *41*, 1.

(25) Scott, A. P.; Radom, L. *J. Phys. Chem.* **1996**, *100*, 16502−16513.

(26) http://srdata.nist.gov/cccbdb/.

(27) Pitzer, K. S.; Gwinn, W. D. J. *J. Chem. Phys.* **1942**, *10*, 428−440.

(28) Lay, T. H.; Krasnoperov, L. N.; Venanzi, C. A.; Bozzelli, J. W.; Shokhirev, N. V. *J. Phys. Chem.* **1996**, *100*, 8240−8249.

(29) Pitzer, K. S. *J. Am. Chem. Soc.* **1946**, *68*, 2209−2212.

(30) Chirico, R. D.; Knipmeyer, S. E.; Nguen, A.; Steele, W. V. *J. Chem. Thermodyn.* **1989**, *21*, 1307−1331.

(31) Baboul, A. G.; Curtiss, L. A.; Redfern, P. C. *J. Chem. Phys.* **1999**, *110*, 7650.

(32) Chase, M. W. *J. Phys. Chem. Ref. Data* **1998**, *9*.

(33) Benson, S. W. *Thermochemical kinetics*, 2nd ed.; Willey: New York, 1976.

(34) Slayden, A. W.; Liebman, J. F. *Chem. Rev.* **2001**, *101*, 1541−1566.

(35) Prosen, E.; Gilmont, R.; Rossini, F. *J. Res. NBS* **1945**, *34*, 65−70.

(36) Streitwieser, A. *Molecular Orbital Theory for Organic Chemists*; Wiley: New York, 1961.

(37) Nagano, Y. *J. Chem. Thermodyn.* **2001**, *33*, 377−388.

(38) Metzger, R. M.; Kuo, C. S.; Arafat, E. S. *J. Chem. Thermodyn.* **1983**, *15*, 841−.

(39) Oja, V.; Suuberg, E. M. *J. Chem. Eng. Data* **1998**, *43*, 486−492.

(40) Nagano, Y. *J. Chem. Thermodyn.* **2002**, *34*, 377−383.

(41) Steele, W. V.; Chirico, R. D.; Nguyen, A.; Hossenlopp, I. A.; Smith, N. K. *AIChE Symp. Ser.* **1990**, 138.

(42) Diogo, H. P.; Persy, G.; Minas, da Pedade, M. E.; Wirz, J. *J. Org. Chem.* **1996**, *61*, 6733−6734.